ELSEVIER

Journal of Power Sources 56 (1995) 87–90

JOURNAL OF POWER SOURCES

Low temperature molybdenum oxide as host lattice for lithium intercalation

Jean-Pierre Pereira-Ramos [a], Naoaki Kumagai [b], Nobuko Kumagai [b]

[a] *C.N.R.S., Laboratoire d'Electrochimie, Catalyse et Synthèse Organique, UMR 28, 2 rue Henri-Dunant, 94320 Thiais, France*

[b] *Department of Applied Chemistry and Molecular Science, Faculty of Engineering, Iwate University, Morioka 020, Japan*

Received 24 December 1994; revised 14 May 1995; accepted 19 May 1995

Abstract

The heat treatment of molybdenum oxide dihydrate resulting from the acidification of Na_2MoO_4 solution leads to various molybdenum trioxides MoO_3. Electrochemical Li insertion into these compounds varies depending on the temperature required for drying the $MoO_3 \cdot 2H_2O$ (250, 400 and 500 °C). The lower the temperature of the heat treatment, the better is the electrochemical performance. The lowest temperature 250 °C induced the formation of a long-range disordered oxide characterized by a high surface area exhibiting the best performance both in terms of specific capacity ($\approx 2F/MoO_3$) and cycling efficiency, which were found to be significantly higher than that usually obtained for the conventional crystalline or amorphous MoO_3 or for the heat-treated form at 500 °C ($\approx 1.5F/MoO_3$). For example, when galvanostatic cycling experiments are performed at a $C/10$ discharge–charge rate within cycling limits 3.8/2 V, ~300 Ah kg^{-1} oxide were still recovered after 10 cycles.

Keywords: Molybdenum oxide; Host lattice; Lithium intercalation

1. Introduction

Orthorhombic molybdenum trioxide, MoO_3, constitutes an interesting host lattice particularly suitable for Li insertion reaction and its application in secondary lithium batteries and electrochromic devices has been suggested [1–6]. Indeed, this oxide exhibits a unique layered structure in which each Mo atom is surrounded by a distorted octahedron of oxygen atoms. Two layers of MoO_6 octahedra sharing all equatorial corners are joined together and stacked one over the other. However, a relative low specific energy of the Li/MoO_3 couple and a poor cycling behaviour are usually reported to be the drawbacks of MoO_3 as a cathodic material.

Recently, some of us outlined interesting features obtained in terms of discharge capacity with molybdenum trioxide hydrates and the molybdic acid C phase prepared through acidification reactions of an aqueous sodium molybdate solution. Depending on the precipitation conditions (concentration of the strong acid, temperature, the presence of cationic species etc.) different phases occur [7,8]. Although high discharge capacities (≈ 400 Ah kg^{-1}), about twice that observed for the classical compound were found [6,7], only low recharge efficiencies which never exceeded 50% were obtained due to important structural changes during cycling.

In the case of tungsten trioxide, we previously demonstrated the interest of using a moderate heat treatment to overcome the instability of the corresponding hydrated compounds and C phase [9,10]. For instance, a considerable improvement both in terms of specific capacity and charge–discharge efficiency was reached by using the hexagonal type oxide $x(A_2O) \cdot WO_3$ ($A = Na^+, K^+, NH_4^+$; $x = 0.05$–0.14) prepared at 350 °C as well as a monoclinic WO_3 with a low degree crystallinity stemming from a drying procedure of H_2WO_4 at 250 °C.

These examples show how much the Li intercalation process depends on the preparation conditions of the host material. Therefore, we have selected a method for producing MoO_3 in order to improve its electrochemical performance. In the present work, we report electrochemical lithium intercalation in orthorhombic molybdenum trioxides obtained from an appropriate heat treatment of MoO_3 dihydrates.

2. Experimental

Molybdenum trioxide dihydrate was prepared according to the method of Freedman [11]. Acidification of a 1 M Na_2MoO_4 aqueous solution with 3 N HCl at 100 °C leads to a yellow powder $MoO_3 \cdot 2H_2O$. Thereafter, a temperature

SSDI 0378-7753(95)02214-2

treatment of $MoO_3 \cdot 2H_2O$ at 250, 400 and 500 °C was carried out in air for 3 h to give MoO_3.

X-ray experiments were performed with an Inel diffractometer using Cu $K\alpha_1$ radiation and the thermal analysis measurements were performed in air at heating rates of 10 °C/min using a Netszch STA 409 analyzer with the simultaneous recording of weight losses (GTA) and temperature variations (DSC).

2.1. Electrochemical measurements

Propylene carbonate (PC) twice distilled (Fluka) was used as received. Anhydrous lithium perchlorate was dried under vacuum at 200 °C for 12 h. The electrolytes were prepared under a purified argon atmosphere. The working electrode consisted of a stainless steel grid with a geometric area of 1 cm^2 on which MoO_3 mixed with graphite (90% by weight graphite) was pressed. Lithium was used as the reference and auxiliary electrode in a flooded cell under an argon atmosphere.

3. Results and discussion

The simultaneously recorded thermal analysis curves (GTA and DSC) of the $MoO_3 \cdot 2H_2O$ powder are shown in Fig. 1. The total weight loss was near 20%, occurring in two successive steps. Thus, the two well defined endothermic peaks correspond to the loss of one water molecule around 100 °C and to that of the more strongly bonded water at 170 °C. No crystallization peak is revealed. Finally, on heating above 200 °C, the anhydrous molybdenum trioxide MoO_3 is obtained.

Chronopotentiometric curves for the reduction at constant current density of $MoO_3 \cdot 2H_2O$ heat treated at different temperatures are reported in Fig. 2. A notable influence of the temperature treatment on the discharge capacity is shown. Indeed, the faradaic yield varies from 1.45 to about 2 Faraday per mole of oxide which corresponds to specific capacities in the range 270–370 Ah kg^{-1}. In the case of the 500 °C heat-treated form, we find the usual electrochemical behaviour

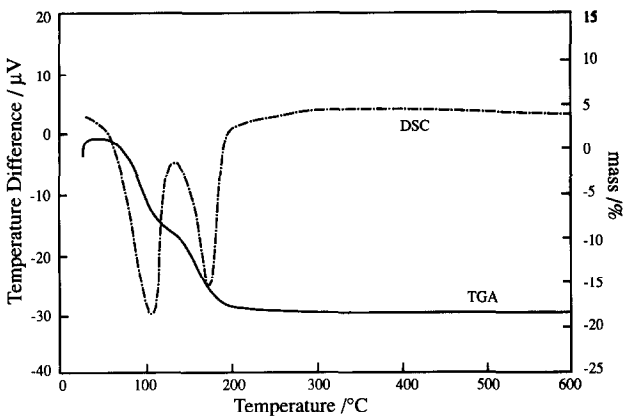

Fig. 1. Simultaneous thermal analysis (TGA and DSC) or $MoO_3 \cdot 2H_2O$.

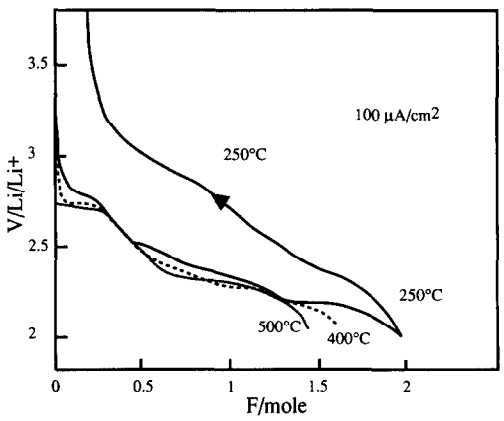

Fig. 2. Comparison of the chronopotentiometric curves for the reduction at constant current (100 $\mu A/cm^2$) of heat-treated $MoO_3 \cdot 2H_2O$ oxides in 1 M $LiClO_4$/PC solution at 20 °C.

reported for the conventional crystalline compounds described in the literature. A well defined reduction process located near 2.8 V, followed by a potential decrease precedes a second longer voltage plateau at 2.3 V. These two reduction steps correspond to a maximum Li uptake of 1.5 Li^+/Mo. However, as shown in Fig. 2, when lower heating temperatures are used, the insertion steps are less defined and give rise to sloping discharge curves around potentials slightly higher than that obtained for the '500 °C' form. The shape of the reduction curve seems to be intermediate between that of crystalline and amorphous MoO_3 [1,2,5]. But, the main interest provided by the procedure involving the lowest temperature consists in the emergence of an additional insertion step at 2.2 V allowing a maximum specific capacity of about 2F/mole of oxide to be reached, i.e. 370 against 280 Ah kg^{-1} for the 500 °C or a commercial sample.

Our results are in accord with those obtained from a thermodynamic investigation of Li insertion in MoO_3 [12] and which led to the possibility of attaining values greater than 1.5Li/MoO_3, in particular 2Li/Mo. A similar high faradaic yield for the reduction process has also been mentioned in the case of crystalline and amorphous porous molybdenum oxides synthesized by reaction of MoO_3 powder with an aqueous H_2O_2 solution at 60 °C and dried in the temperature range 170–400 °C [13]. In addition, both the working potential and the capacity are greatly improved even in respect to the amorphous phases MoO_3 ($x_{max} \approx 1$ for a cut off voltage of 2 V) synthesized via precipitation techniques involving the dissolution of the crystalline form in ammonia followed by an acid treatment using nitric acid [5].

X-ray diffraction patterns in reflection geometry of the different heat-treated forms are summarized in Fig. 3. The lowest temperature '250 °C' leads to a phase which seems to be amorphous, whereas the patterns of the 400 and 500 °C forms can be indexed on the basis of an orthorhombic structure with the usual lattice parameters [14]. X-ray diffraction patterns of MoO_3 prepared at 400 °C exhibit broader diffractions peaks significant of a lower degree of crystallinity than in the case of the '500 °C' oxide. However, the formation of

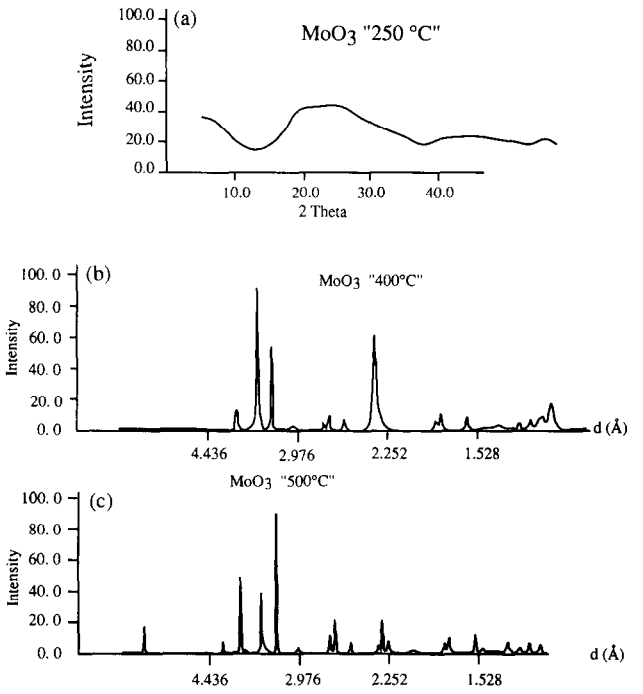

Fig. 3. Comparison of the X-ray diffraction patterns (Cu $K\alpha_1$) of the molybdenum oxides MoO_3 obtained at 250, 400 and 500 °C.

a long range disordered phase at '250 °C' rather than a really amorphous compound MoO_3 would be more consistent with its electrochemical behaviour characterized by defined steps and at the same time by a sloping discharge curve as also confirmed by voltammetric measurements (Fig. 4). This is significantly different from the S-shaped curves reported for a-MoO_3 [5].

An additional information can be drawn from the voltammetric curve of the '250 °C' compound (Fig. 4). Even when the reduction curve seems to include different subsequent insertion processes due to the appearance of four cathodic peaks at 2.75, 2.43, 2.30 and 2.05 V, the coulombic efficiency for the oxidation reaction is high in the order of >90%.

The influence of the current density on the discharge–charge of MoO_3 synthesized at 250 °C is reported in Fig. 5. No significant effect on the working potential is shown. Only a low decrease of the faradaic yield is pointed out when the current density varies from 100 μA to 1 mA cm^{-2}. Secondly, MoO_3 '250 °C' exhibits a highly rechargeable behaviour (90%) while a poor efficiency which never exceeds 60% is commonly reported for the usual crystalline MoO_3 ($x_{max} \approx 1.5$) [2]. Nevertheless, a recent paper outlines the possibility of charging MoO_3 cathodes also with a high efficiency during the first ten cycles using a $C/20$ discharge–charge rate [15].

In agreement with a similar effect recently encountered in the case of WO_3 [9] and as indicated from BET measurements summarized in Table 1, the lower the temperature treatment, i.e. the lower the degree of crystallinity, the higher the active area and the specific capacity.

Indeed, the smaller particles of the sample prepared at 250 °C allow a considerable enhancement of the active area (32 m^2/g), by a factor of ten, to be obtained and then of the electrochemical surface area involved in the discharge–charge process. In this way, lithium overconcentrations at the surface of the material are probably minimized.

Thus, the potential interest of the low temperature oxide characterized by a maximum specific capacity of 370 Ah kg^{-1} and the promising efficiency of the charge process prompted us to evaluate the cycling properties of this material in comparison with the other heat-treated solids. Fig. 6 shows the evolution of the mass capacity as a function of cycle number for three kinds of compounds. Whatever the discharge–charge rate, the '250 °C' sample gave the best results. Lithium insertion in crystalline MoO_3 is known to induce important structural changes. Unlike in Li_xTiS_2 or Li_xMoS_2, the lattice expansion in Li_xMoO_3 does not increase continuously with x: an important increase of the interplanar distance occurs and shows a maximum close to about $x=0.5$ (5%), followed by a significant contraction ($\sim$10%) from $x=0.5$

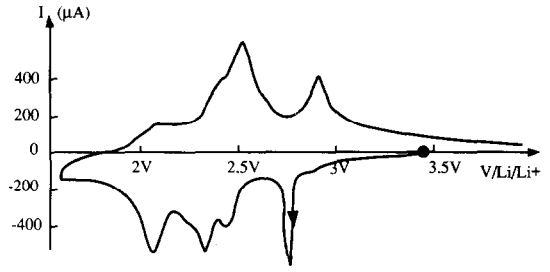

Fig. 4. Voltammograms of an MoO_3 '250 °C' electrode in 1 M $LiClO_4$/PC at 20 °C. The scanning speed was 2×10^{-4} V s^{-1}.

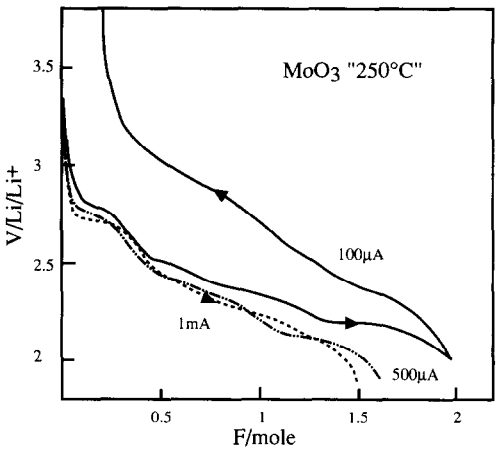

Fig. 5. Influence of the current density on the discharge–charge curves of MoO_3 synthesized at 250 °C.

Table 1
BET surface areas of various MoO_3 powders

Materials	Surface area (m^2/g)
'250 °C' MoO_3	32.3
'400 °C' MoO_3	11.5
'500 °C' MoO_3	1.9

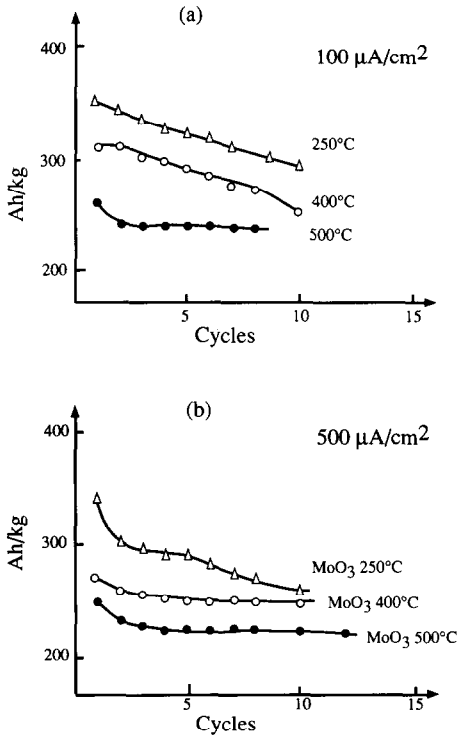

Fig. 6. Variation of the mass capacity as a function of cycle number for MoO_3 prepared at 250, 400 and 500 °C: (a) 100, (b) 500 $\mu A\ cm^{-2}$ (cycling limits 3.8/2 V).

up to 1.4 [3]. The peculiar shape of the '250 °C' oxide showing a more regular, although stepped, discharge curve could indicate a less severe structural reorganization which would explain the better rechargeability of this compound. The disordered state of the material combined with the small grain size or a high porosity deduced from BET measurements, should make it easier for the material to accommodate important volume changes occurring in the Li_xMoO_3 phases.

Starting from an initial value of about 340 Ah kg^{-1} obtained at a discharge–charge rate of $C/10$, the specific capacity continuously decreases with cycling (Fig. 6(a)). However, after the tenth cycle about 300 Ah kg^{-1} are still available against only 240 Ah kg^{-1} in the case of conventional MoO_3. For a higher discharge–charge rate ($C/2$; Fig. 6(b)), the main discrepancies between the compounds remain but are not so strongly pronounced. Indeed, the capacity of the '250 °C' MoO_3 is more affected and significantly decreases to reach that of the classical compounds, which suggests the occurrence of structural modifications.

Finally, Fig. 7 shows that at a lower discharge–charge rate $C/20$, the specific capacity slowly decreases to remain stable

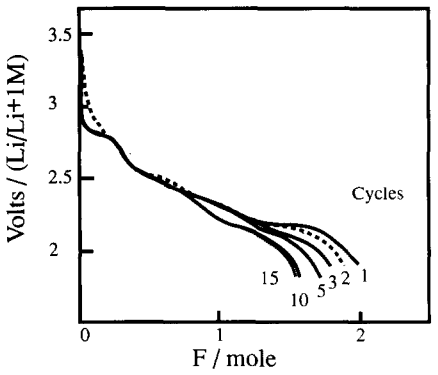

Fig. 7. Evolution of the discharge curves of MoO_3 '250 °C' during galvanostatic cycling experiments ($C/20$ rate).

for at least 10 cycles. Thus, as mass capacity of 300 Ah kg^{-1} is still recovered after 15 cycles.

Besides the favourable effect on the electrochemical behaviour afforded by the enhancement of the active surface area, other possible parameters like oxygen stoichiometry, or the presence of interstitial hydrogen or residual water could be also responsible for the observed differences, and cannot be discarded. Further work is still needed to elucidate the responsible mechanism.

References

[1] L. Campanella and G. Pistoia, *J. Electrochem. Soc., 118* (1971) 1905.
[2] J.O. Besenhard and R. Schöllhorn, *J. Power Sources, 1* (1976/77) 267.
[3] J.O. Besenhard, J. Heydecke and H.P. Fritz, *Solid State Ionics, 6* (1982) 215–224.
[4] J.O. Besenhard, J. Heydecke, E. Wudy, H.P. Fritz and W. Foag, *Solid State Ionics, 8* (1983) 61.
[5] F. Bonino, L. Peraldo Biceli, B. Hivolta, M. Lazzari and F. Festorazzi, *Solid State Ionics, 17* (1985) 21.
[6] J. Labat, V. Dechenaux, Y. Jumel and J.P. Gabano, *172nd Meet. Electrochemical Soc., Honolulu, HI, USA, 1987*, p. 86.
[7] N. Kumagai, N. Kumagai and K. Tanno, *Electrochim. Acta, 32* (1987) 1521.
[8] N. Kumagai, N. Kumagai and K. Tanno, *J. Appl. Electrochem., 18* (1988) 857.
[9] R. Baddour, J.P. Pereira-Ramos, N. Kumagai and K. Tanno, *Electrochim. Acta, 38* (1993) 431.
[10] N. Kumagai, Y. Matsuura, N. Kumagai and K. Tanno, *J. Electrochem. Soc., 139* (1992) 3553.
[11] M.L. Freedman, *J. Am. Chem. Soc., 81* (1959) 3834.
[12] M. Pasquali, F. Rodante and G. Pistoia, *Thermochim. Acta, 121* (1987) 203.
[13] M. Sugawara, Y. Kitada and K. Matsuki, *J. Power Sources, 26* (1989) 373.
[14] ASTM, *Powder Diffraction File No. 5-0508.*
[15] M.E. Spahr, P. Novak, O. Haas and R. Nesper, *7th Int. Meet. Lithium Batteries, Boston, MA, USA, 15–20 May 1994*, p. 497.